DNA functionalized spider silk nanohydrogels for specific cell attachment and patterning

DNA Functionalized Spider Silk Nanohydrogels for Specific Cell Attachment and Patterning

Christina Heinritz, ⊥ Zan Lamberger,⊥ Karolína Kocourková, Antonín Minařík, and Martin Humenik*

Christina Heinritz - Department of Biomaterials, Faculty of Engineering Science, Universitat Bayreuth, 95447 Bayreuth, Germany

Zan Lamberger - Department of Biomaterials, Faculty of Engineering Science, Universitat Bayreuth, 95447 Bayreuth, Germany; Present Address: Department of Functional Materials in Medicine and Dentistry, University of Wu "rzburg, Pleicherwall 2, 97070 Wu "rzburg, Germany

Karolína Kocourková - Department of Physics and Materials Engineering, Tomas Bata University in Zlín, 76001 Zlín, Czech Republic

Antonín Minařík - Centre of Polymer Systems, Tomas Bata University in Zlín, 76001 Zlín, Czech Republic; Department of Physics and Materials Engineering, Tomas Bata University in Zlín, 76001 Zlín, Czech Republic

Corresponding author: Martin Humenik - Department of Biomaterials, Faculty of Engineering Science, Universitat Bayreuth, 95447 Bayreuth, Germany, Email: martin.humenik@bm.uni-bayreuth.de

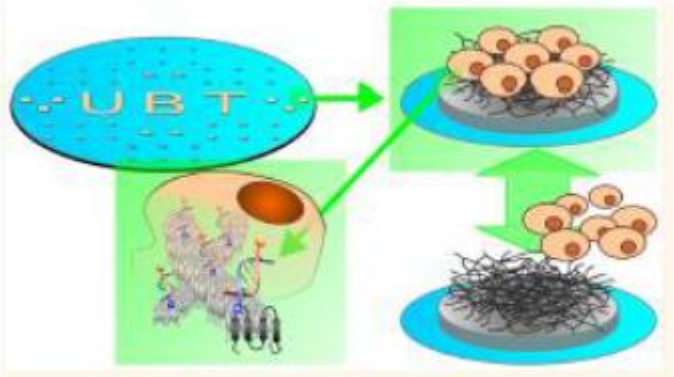

ABSTRACT

Nucleated protein self-assembly of an azido modified spider silk protein was employed in the preparation of nanofibrillar networks with hydrogel-like properties immobilized on coatings of the same protein. Formation of the networks in a mild aqueous environment resulted in thicknesses between 2 and 60 nm, which were controlled only by the protein concentration. Incorporated azido groups in the protein were used to "click" short nucleic acid sequences onto the nanofibrils, which were accessible to specific hybridization-based modifications, as proved by fluorescently labeled DNA complements. A lipid modifier was used for efficient incorporation of DNA into the membrane of nonadherent Jurkat cells. Based on the complementarity of the nucleic acids, highly specific DNA-assisted immobilization of the cells on the nanohydrogels with tunable cell densities was possible. Addressability of the DNA cell-to-surface anchor was demonstrated with a competitive oligonucleotide probe, resulting in a rapid release of 75-95% of cells. In addition, we developed a photolithography-based patterning of arbitrarily shaped microwells, which served to spatially define the formation of

the nanohydrogels. After detaching the photoresist and PEG-blocking of the surface, DNA-assisted immobilization of the Jurkat cells on the nanohydrogel microstructures was achieved with high fidelity.

KEYWORDS: Self-assembly, nanofibrils, nanohydrogels, DNA modification, cells, surfaces, patterning

Materials scientists face challenges in fabricating artificial biomaterials that effectively mimic cell interactions as provided by a native extracellular matrix (ECM) with entire macro-, meso- down to nanofibrous architectures. Thus, to prepare such biocompatible scaffolds for a full tissue regeneration, a plethora of requirements have to be fulfilled, such as adequate mechanical and structural support, control of cell attachment, migration, proliferation and differentiation as well as appropriate bioresorbable features to allow the body to heal itself at the same rate as implant degradation.[1-3] Conventional approaches which use bulk materials and modifications thereof are rather laborious in screening the huge amount of potential material parameters to identify the optimal cellular responses. To speed up the process, platforms for material—cell interactions have been developed in the case of synthetic polymers, peptides, ECM components, or polysaccharides.[3-6] The resource efficient approaches of culturing and analyzing cells via position-specific immobilization employed microtiter plates,[7-9] high-density spotting,[10-13] microfabrication,[14-17] or microfluidic technologies.[18,19] Involvement of living-cell assays on the cell microarrays requires a stable attachment of cells, inert surfaces which do not interfere with cultivated cells and are stable in contact with cultivation media as well as upon steriliza-tion.[20-22] DNA-assisted immobilization on patterned surfaces could be applied for cell immobilization regardless of the cell type,23-25 to program cell-surface and cell-cell adhesion with high position fidelity to study complex cell biology on the 2D[26-28] and 3D level,[29] but the technology was not involved in studies of screening platforms for material-cell interaction yet.

Biopolymer nanofibrils exhibit a combination of strength and toughness, while also capable of presenting biological fUnctions.[30,31] Such fibrous systems, morphologically rendering [a](A) Molecular structures and schematic representations of the lipid, DBCO, and azido moieties, which were used for modification of the DNA strands, spider silk protein and cells. (B) The azido modified spider silk protein self-assembled into fibrillar networks on a spider silk pattern defined by a photolithography. Employing the coupling of DBCO-oligonucleotides to the azide-nanohydrogel and incorporation of the complementary lipid-oligonucleotides into the cellular membrane, immobilization of the cells on the micropatterned nanohydrogels could be achieved via highly specific DNA interactions.

ECM, likely form hydrogel networks which are the preferred material morphology to interact with cells in tissue engineering applications.[32] We have shown that recombinant variants of spider silk proteins self-assembled into nanofibrils via a nucleation mechanism specifically triggered by phosphate ions in a mild milieu[33,34] and tolerated a wide range of genetical[35] or chemical[36,37] modifications. Generally, the recombinant spider silk proteins and materials made thereof are noncytotoxic, nonimmunogenic, and degradable,[38,39] thus representing a highly suitable biomaterial for tissue engineering applications.[40] Recently, we introduced chemically modified DNA-spider silk conjugates which enabled a combination of the protein self-assembly into fibrils and the programmability of DNA hybridization into hierarchically organized hybrid materials.[36,37,41] Redirection of the protein fibrillization via nucleation onto surfaces of the same protein[34] resulted in the development of immobilized fibrillar networks with nanohydrogel properties and an aptameric functionality, which enabled accommodation of sensitive biologicals as well as controlled release thereof.[4,42]

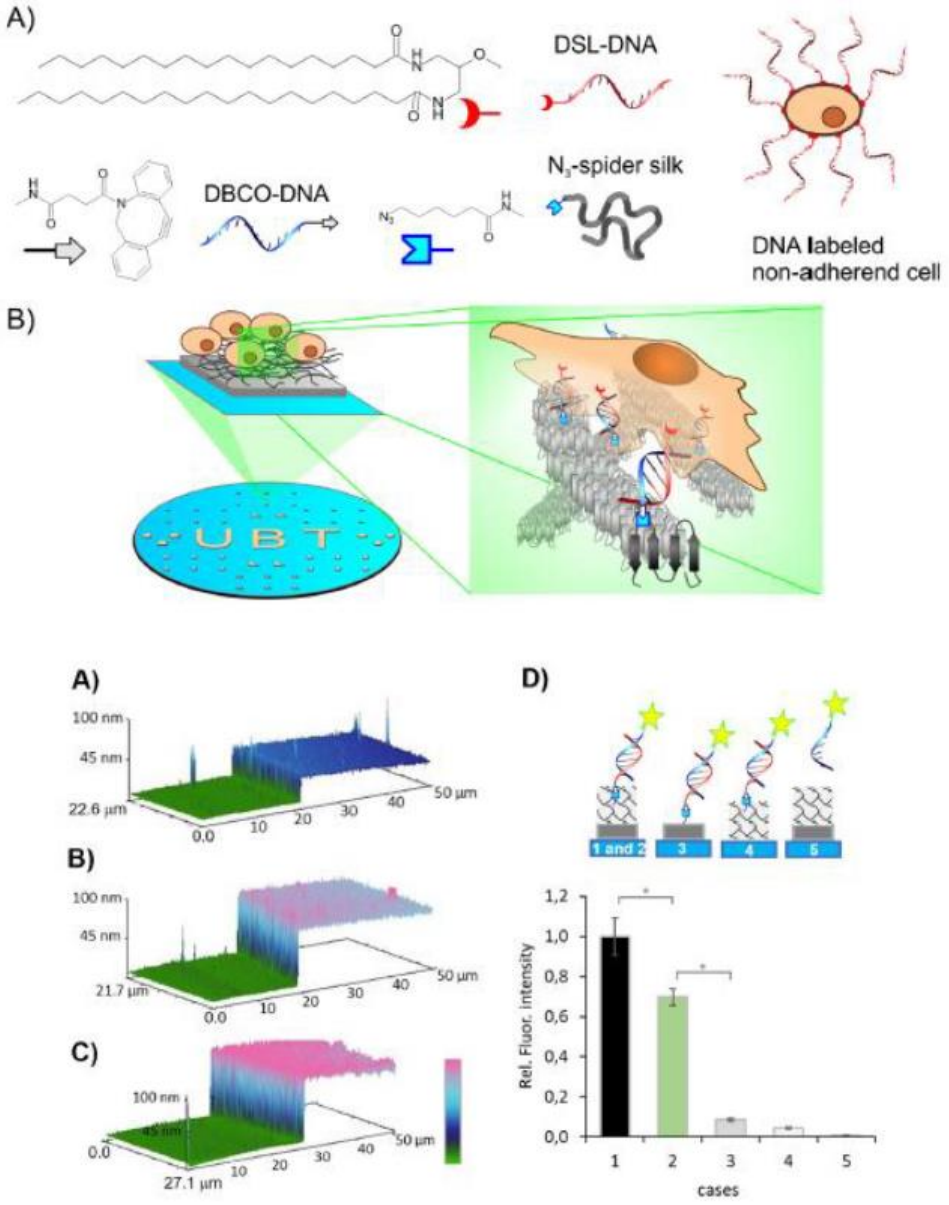

Figure 1. Characterization of self-assembling nanohydrogels. (A-C) Representation of nanohydrogel heights assembled from 2, 5, and 10 μM N_3-eADF4(C16) resulting in 2, 43, and 56 nm-thick fibrillar networks on a 36 nm thick film layer of eADF4(C16) (**Table S1**), respectively. (D) In the upper panel the studied cases are represented schematically. (1) Nanohydrogel (nh) directly assembled from the rep-eADF4(C16) conjugate on the eADF4(C16) nanofilm (nf); (2) N_3-eADF4(C16) nh on eADF4(C16) nf functionalized by DBCO-rep after the assembly; (3) N_3-eADF4(C16) nf only; (4) N_3-eADF4(C16) nh only; and (5) eADF4(C16) nh on eADF4(C16) nf (5). In the lower panel, amounts of surface presented rep-sequence (red) in the reaction setups (1-5) were compared after the hybridization of a complementary probe FAM-cap (blue). Color bar from -10 to 100 nm in (A-C).

Herein, we utilized the surface-controlled spider silk selfassembly to develop "click" nanohydrogels as a biomaterial platform suitable for microfabrication techniques to create distinct nanohydrogel patterns on surfaces and enabling versatile functionalization with nucleic acids (**Scheme 1**). We demonstrated that the DNA-spider silk nanohydrogels represent environmentally robust and biocompatible surface modification with low cell adhesion properties allowing highly specific cell immobilization and release upon DNA-specific interactions in well and microarray formats.

RESULTS AND DISCUSSION

Nucleic Acid Functionalized Nanohydrogels. Previously, we have shown that the conjugates of the recombinant spider silk protein eADF4(C16) with short single-stranded DNA aptamers directly assembled into the DNA-functionalized nanohydrogels.[42] Herein, the functionalization was induced in a postassembly approach. In the first step, N_3-eADF4(C16), a recombinant spider silk protein selectively modified by an azide containing tether on the N-terminus,[36] was assembled on top of nonfunctionalized eADF4(C16) films, applying a surface seeding mechanism.[34,42] AFM analysis revealed an increasing thickness of the nanofibril networks with the increasing protein concentration (**Figure 1**A-C). Interestingly, the increase was not proportional, as nanohydrogel thickness showed a 23.8-fold increase in the case of nanohydrogel assembled from 2 μM vs 5 μM and only 1.3-fold increase in case of assembly at 5 μM vs 10 μM (**Table S1** and **Figure S1**). The fibril formation is a nucleation-dependent process starting with a slow lag phase, the duration of which is strongly dependent on protein concentration. Once the nuclei are formed, fibril growth in solutions tends to be rapid and less sensitive to the monomer concentration.[34] Therefore, it is likely possible that the self-assembly on surfaces at 2 μM protein was still in the lag phase after 24 h of incubation, while 5 and 10 μM proteins have already reached the end of the process. Despite the significant height differences of the nanohydrogels, the roughness analyses showed rather similar values (**Table S1**), suggesting uniform assembly of the protein on the even nanofilm.

In the second step, the N_3-nanohydrogel functionalization was achieved using short dibenzocyclooctin (DBCO) modified oligodeoxynucleotides[42] in a strain-promoted azide—alkyne cycloaddition.[43] Coupling of the modified capture sequence (DBCO-cap) on the azido nanohydrogel was examined via fluorescein-phosphoramidit-labeled complementary reporter sequence FAM-rep (**Figure S2**). The coupling yield was directly proportional to the employed DBCO-cap concentration (**Figure S2B**) in the concentration regime 1 — 10 μM. The slow reaction kinetic extended the reaction time from 48 h in a homogeneous solution[42] to 72 h for the heterogeneous coupling to the solid support even at elevated temperature (37 °C). The postassembly functionalization of the spider silk fibrillar network was further compared to alternative modification setups (**Figure 1**D, cases 1—5). The nanohydrogels assembling directly from the conjugate rep-eADF4-(C16) (case 1) exhibited the highest density of accessible DNA strands in comparison to the postassembly coupling on N_3-eADF4(C16) nanohydrogels, which yielded a slightly lower capacity (case 2, 70%). However, the postassembly modification strategy overcame the time-consuming preparation of the DNA-spider silk conjugates,[36,42] which can be especially valuable in multiplex approaches where a plethora of binding sequences, such as aptamers, could be tested. Two other morphologies, azide modified films (case 3) as well as N_3-eADF4(C16) nanohydrogels without the underlying spider silk film (case 4), showed a very low fluorescence of 8% and 5%, respectively, highlighting two important aspects. First, the benefit of employing a nanofibrillar network instead of a plain film, due to a significantly larger surface area presented on the nanofibrils which could be exploited for the exposition of functional groups. Second, the importance of the eADF4(C16) film as a basis for the hydrogel immobilization via the nucleating nanofibril assembly.[42] Noteworthy, the fluorescein-labeled detection probe showed no unspecific binding on unmodified eADF4(C16) nanohydrogels (case 5).

Modification of the Cell Membrane with SingleStranded DNA. To test suitability of the DNA-modified nanohydrogel surfaces for selective immobilization of cells, we modified the cell membrane of nonadherent Jurkat T-cells with a complementary sequence. The spontaneous insertion of an amphipathic lipid[29,44,45] was chosen as a mild, straightforward, rapid, and efficient process applicable

across multiple cell types.[46] For this purpose, the insertion of a commercially available distearoyl-lipid 5' modification with the rep sequence (DSL-rep) was examined (**Figures 2**, **S3**, and **S4**).¨

To establish the procedure, the impact of DSL-rep concentration as well as the incubation times on the incorporation efficiency were analyzed using flow cytometry and the fluorescently labeled complementary capture sequence (carboxy-tetramethylrhodamin TAMRA-cap) (**Figures 2** and **S3A**). Kinetics of the DNA-lipids insertion into membranes were shown in literature as a time-dependent saturation.[46] Here, the examined progression of the insertion did not show a similar maximum threshold (**Figure S3A**); however, to keep the cell stress at a minimum, the shortest time (5 min) showing significant increase in labeling degree (60% in comparison to 30 min) was chosen for the cell incubation. Another important issue, the persistence of the DNA modification in the plasma membrane was examined as well. Already within the first hour, a drop of approximately 80% of the membrane modification was indicated (**Figure S3B**). As discussed in literature, the instability of lipid-DNA modifications is caused either by their release into the surrounding medium or internalization into the cell,[45,47] whereas factors such as temperature48 or hydrophobicity of the lipid moiety46 influence this process. Indeed, the lipid-DNA labeling density declined slower at 4 °C in comparison to the room temperature and to 37 °C.

The density of DNA incorporated into the cells apparently increased with the increasing concentration of DSL-rep, as visualized in **Figure 2**B—E. However, nonhomogeneous distributions of the DNA modification in the cell populations have been noticed from the micrographs and were further confirmed by flow cytometry, showing an overall broad signal distribution in the concentration regime between 0.5 and 20 μM of DSL-rep (**Figure 2**F). Quantification of the TAMRA-cap fluorescence intensities revealed a linear increase in DSL-rep labeling densities (**Figure 2**G). Hence, the utilization of the lipid-DNA in micromolar range enabled adjustment of the modification degree of the cells, whereas the viability of the cells was not concentration dependent and in the range of nonlabeled cells (**Figure S4**).

DNA-Assisted Immobilization and Triggered Release of Cells. To test the specificity of the DNA modified spider silk nanohydrogels in DNA-assisted cell binding, rep-cells were applied on cap-nanohydrogels. The nonadherent Jurkat cell line was ideal to test the stringency of the immobilization specificity, as possible interactions with the nanohydrogel surface could be related directly to the specific rep/cap hybridization, instead of other cellular effects supporting surface-cell interactions in case of adherent cells.[49] The incubation of rep-cells on cap-nanohydrogels for 30 min resulted in a dense cell distribution after washings (**Figure 3**A). In contrast, native Jurkat cells showed negligible unspecific interaction on DNA-functionalized as well as unmodified eADF4(C16) nanohydrogels (**Figure 3**C,D), similarly to the DNA-modified rep-cells on the nonfunctionalized nanohydrogels (**Figure 3**B).

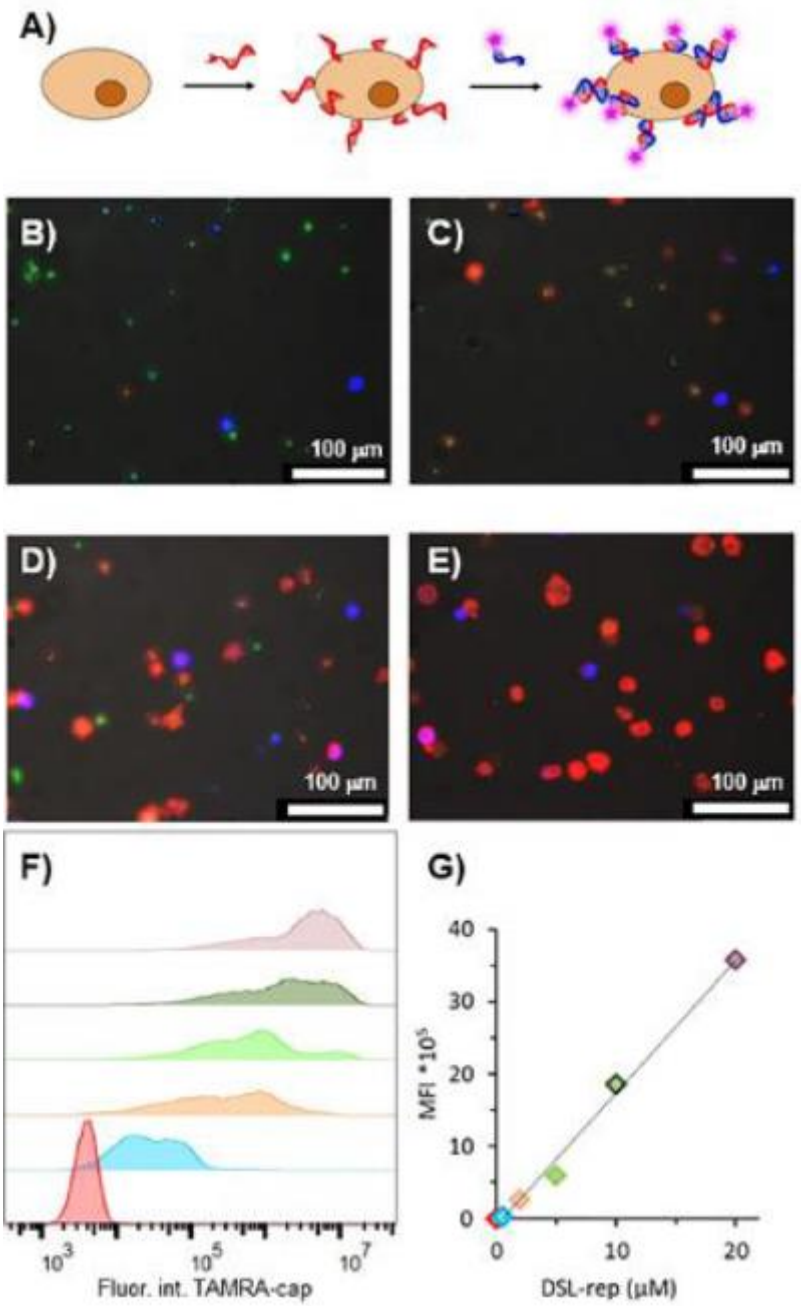

Figure 2. Analysis of DSL-DNA incorporation into cells. (A) Schematic representation of the cell membrane modification using DSL-rep sequence (red) and detection of the modification via hybridization with the complementary sequence TAMRA-cap (blue). Fluorescence micrographs of Jurkat cells after treatment with 0.5, 2, 5, and 10 μM DSL-rep in (B-E), respectively, after staining with live stain calcein-AM (green), nuclei stain DAPI (blue), and rep sequence specific stain TAMRA-cap (red). The fluorescence intensities of nonlabeled control cells (red), 0.5 μM (blue), 2 μM (orange), 5 μM (light green), 10 μM (dark green), and 20 μM (violet) DSL-rep labeled cells were analyzed after the hybridization of TAMRA-cap using flow cytometry in (F) and evaluated as median fluorescence intensities (MFI) in (G).

Additionally, we designed cap-based sequences containing one to three mismatched base pairs to assess the importance of the hybridization fidelity and potential additional non-DNA-based effects which could influence the cell-nanohydrogel interactions (**Figure S5**). Whereas the DNA-assisted immobilization was not sensitive to the presence of one mismatch (Figure S5A vs B), already two and three mismatches reduced the cell densities significantly to the low background levels (Figure S5C,D vs E). Importantly, the fidelity of the complex system, the multivalent DNA-based cell-nanohydrogel

interactions in cell culture media, corresponded well with the simple model of monovalent FAM-rep binding in Tris/NaCl buffer (**Figure S5**F vs G). These experiments confirmed that the DNA recognition is fundamental for the DNA-assisted binding, and potential unspecific interactions between the cell surface, and the spider silk protein-based nanohydrogels in the complex biomacromolecule system are negligible. The high specificity of the cell-nanohydrogel binding represents a very important prerequisite for the selection of the substrates employable in high-throughput live cell arrays.[26]

As the higher labeling concentration of DSL-rep caused an increased density of DNA modifications (**Figure 2**), correspondingly the higher probability of hybridization events between rep-cells and cap-nanohydrogels resulted in increasing density of the immobilized cells (**Figure 3**I, cases 1-3, black bars), whereas lack of the specific rep/cap anchorage resulted in negligible cell counts (**Figure 3**I, cases 4 and 5), confirming the observation from the micrographs (**Figure 3**A-D).

Generally, in DNA hybridization pairs, one of the strands can be replaced by a strand possessing an extended complementary region (**Figure 3**F), making the binding energetically more favorable.50 Hence, a fluorescein-labeled competitive probe (FAM-cap-comp) was successfully tested in the exchange of TAMRA-cap in solution (**Figure S6**) as well as on rep-cells in suspension (**Figure 3**G,H) and used to release the rep-cells from the cap-nanohydrogel (**Figure 3**I, cases 1-3, green bars), showing significantly decreased cell densities. Whereas more than 93% of rep-cells at the low surface density (0.5 ,jUM DSL-rep, case 1) were released, at higher cell labeling concentrations, 86-78% of the rep-cells were washed away (cases 2 and 3, respectively).

Extension of the cap-comp incubation resulted in no significant difference in the release efficiency (**Figure S7**). Moreover, comparison with the control group (medium) indicated that short-term release ($<$1 h) is triggered specifically by the strand displacement, whereas for longer times ($>$1 h), the decrease in immobilized cells density was also due to an unspecific detachment, as in absence of the cap-comp probe only 59% after 2 h and 35% cells after 4 h was presented on the surface. The steady cell detachment might result from the loss of the lipid-DNA due to dynamic remodeling of the lipid membrane, internalization, or even degradation by a nuclease activity[51,52] and corresponds also with the decrease of DNA labeling density on the cell in suspension, as demonstrated in **Figure S3**B. However, if required, a stabilization of oligonucleotides in the membrane could be achieved by lipid anchor derivatives, helper oligonucleotides, or cholesterol-based modifiers.[44-46] For example, the lipid and cholesterol modifier showed very similar effectiveness in the Jurkat cell's modification and DNA-assisted immobilization (**Figure S5**F). In the future, it would be possible to exchange the artificial DNA cell-surface anchor with, e.g., aptamer- or antibody-to-cell membrane marker interactions, which could be more suitable for a long-term cell incubation, whereas still providing a cell type addressability.

The morphology of the specifically immobilized Jurkat cells was further analyzed by confocal laser scanning microscopy (CLSM). After the immobilization, the rep-cells were fluorescently labeled using TAMRA-cap to target remaining free rep sequences on the cell surfaces. The series of CLSM images in **Figure 3**E showed formation of short filopodia, i.e., extended actin-filaments inside membrane protrusions[53] on the cell-nanohydrogel interface (E1 and E2). The formation of such filopodia in case of the suspension cells is consistent with the observations in vivo, where circulating T-cells are activated by stimulation of various surface proteins, leading inter alia to T-cells adhering to the vessel epithelium and migrating into the surrounding tissues for exertion of the immune response.[53,54] Along with these processes, the cytoskeleton is rearranged, enabling adhesion, spreading, and the formation of filopodia.[53]

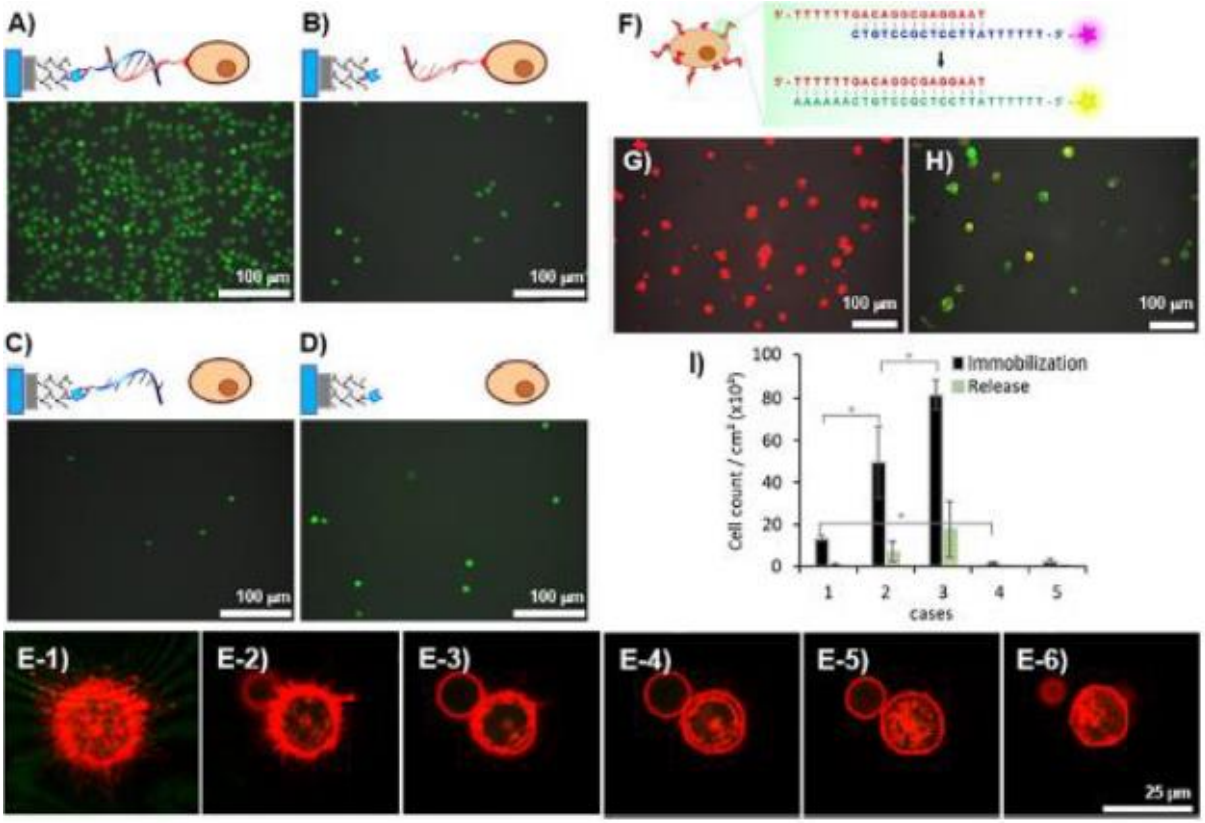

Figure 3. Performance of DNA-functionalized nanohydrogels in the DNA-assisted immobilization and release of cells. (A-D) Comparison of fluorescence micrographs of DSL-rep labeled in (A and B) and unmodified cells in (C and D) after live staining on the cap modified in (A and C) and the unmodified eADF4(C16) nanohydrogels in (B and D). For confocal microscopy in (E), the cells modified with 15 DSL-rep were immobilized as in (A), and unoccupied rep-strands were labeled with the complementary TAMRA-cap (0.5 μM). The cross sections were performed with a z-stack distance of 2.88 fim from the bottom to the top (E1-E6). (F) Strand displacement principle replacing the shorter rep/cap hybridization (red/blue) with the longer rep/cap-comp (red/green) via (T)6 overhangs was applied on the cells to label the rep-cells in suspension in the presence of TAMRA-cap (red fluorescence) in (G) and upon addition of FAM-cap-comp in (H) to show predominant binding of the green fluorescent competitive probe on the surface of rep-cells. (I) Cell densities of the immobilized cells as evaluated from fluorescence micrographs obtained after the immobilization (black bars) and release (green bars), respectively, in cases of cells modified with 0.5, 2, and 5 μM DSL-rep and immobilized on the cap-nanohydrogels (1-3) as well as 5 iM DSL-rep modified and native cells on unmodified nanohydrogels (4 and 5), respectively. The release in cases 1-3 was triggered by incubation of the competitive cap-comp probe for 30 min.

The diameter of the cell was increased at the cell base if compared to higher stacks from E-1 to E-6, indicating cell flattening. The TAMRA-cap labeling on the rep-cells revealed granular structures in the membrane visible at the base (E-1) as well as on the upper part of the cells (E-5) evoked most probably due to the inherent clustering of membrane lipids and proteins.[55]

Patterning of Nucleic Acid Modified Cells. Photolithography could be used to pattern different types of macromolecules on surfaces or in thin hydrogel layers[56] to trigger and control cell-surface interactions. Direct patterning of DNA strands has been shown as a valuable approach in creation of microenvironments consisting of different cells and cellular signals.[26,27] Herein the concept of DNA-assisted cell immobilization was further challenged on patterns made of spider silk nanohydrogels via maskless digital projection photolithography (**Figure 4**A) to establish a microstructured biomaterial

platform. For this, amino-activated glass substrates were used in a combination with a positive-tone photoresist to define arbitrarily shaped microwells 50-200 μm in diameter and 1 μm in depth as characterized with optical (**Figures 4**B and **S8A**) and contact profilometry (**Figures 4**C and **S8B**,**C**).

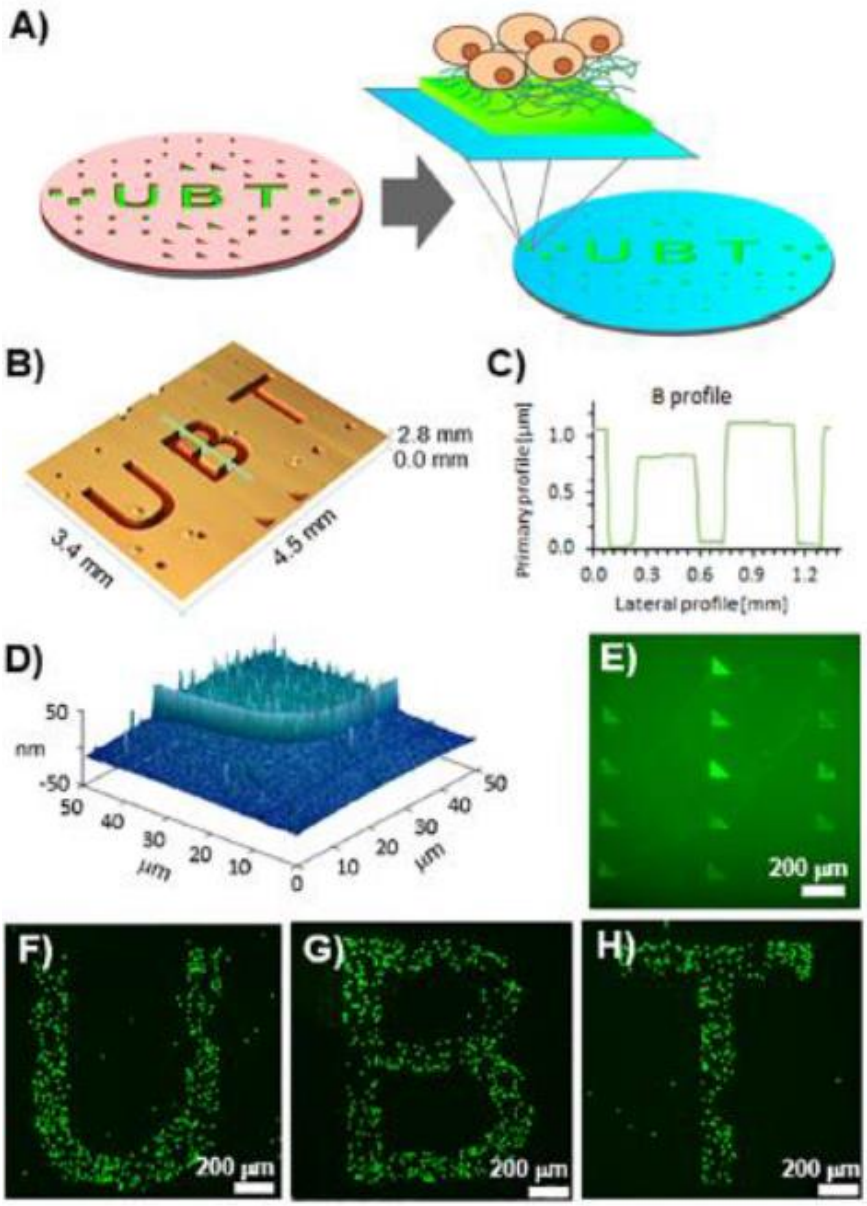

Figure 4. DNA-assisted cell immobilization on micropattern. (A) Schematic representation of the micropatterning approach using a positive-tone photoresist (reddish) enabling the creation of microwells for spatially defined immobilization and selfassembly of the DNA-modified nanohydrogels (green), which could be exposed after the photoresist stripping on a PEG-blocked surface (pale blue) to the binding of DNA-labeled cells. (B) Optical profilometry image of the microshaped wells obtained in the photoresist after positive-tone photolithography. (C) Crosssectional profile of the B-well. (D) AFM scan of a nanohydrogel micropattern corner after photoresist stripping. (E) Fluorescence micrograph of the microshaped nanohydrogels obtained after photoresist stripping, modification with NH_2-cap sequence, and hybridization of the complementary FAM-rep probe. (F-H) DSL-rep modified Jurkat cells immobilized on the letter shaped cap-nanohydrogel micropattern in a fluorescence microscope after live staining.

After the pattern irradiation and development of the photoresist, the amine-exposed bottom of the microwells enabled chemical immobilization of the unmodified eADF4-(C16). The covalently coupled

protein layer was exploited as a nucleation site for the subsequent position specific selfassembly of the fibrillar networks from the same protein. To increase the density of the nucleic acid strands in the microspace to a maximum, 5'-amino modified capture DNA was then coupled to the nanohydrogels exploiting N-(3-dimethylaminopropyl)-N'-ethylcarbodiimid-hydrochlorid (EDC) activation of the abundant glutamic acid residues (16 per the protein sequence). Finally, the DNA-modified nanohydrogel micropatterns were cleared of the photoresist using stripping in organic solvents, and the unveiled amino modified glass surface was blocked using NHS-activated branched PEG. The AFM scans showed the presence of the well-defined nanohydrogel edges with heights between 10 and 20 nm (**Figures 4**D and S9A,B), which were, however, lower in comparison to the nanohydrogels assembled in the open system of Si-wafers (**Figure S1**, **Table S1**, at 5 μM protein). It is possible that the harsh photoresist stripping procedure caused partial disassembly of the nanohydrogel upper layers. Importantly, the stripping procedure did not affect the shape of the resulting nanohydrogels micropatterns as well as the functionality of the DNA modifier, as shown exemplarily on the cap-nanohydrogels after the hybridization of complementary FAM-rep strand (Figure 4E). Thus, the micropatterns were used in the cell immobilization procedure employing rep-cells. After 1 h incubation and washings, the cell localization was visualized using fluorescence microscopy after live staining (**Figures 4**F-H and **S9C-F**) and AFM scans (**Figure S9G,H**), showing clear binding preference of the DNA-modified cells to the correspondingly DNA-modified nanohydrogel micropattern. In case of the nanohydrogel pattern made of the unmodified spider silk protein, the unmodified as well as rep modified cells were easily washed off (not shown). Nanohydrogel microstructures such as the letters U, B, and T (**Figure 4**F-H), triangles as well as squares (**Figure S9D-F**) demonstrated well shape fidelity of cell-nanohydrogel structures down to 50 μm in diameter. The AFM scans revealed the cells remaining strictly inside the micropattern borders, i.e., high preference toward specifically provided DNA-assisted binding, which was supported by the nonfouling properties of the surrounding PEG surface.

CONCLUSIONS

The presented study shows development of immobilized selfassembling fibrillar networks from the recombinant spider silk protein eADF4(C16) into fibrillar networks of variable thicknesses from 2 to 60 nm. Introduction of an azide linker in the self-assembling protein allowed further functionalization of the nanohydrogels with DBCO-modified nucleic acid sequences via bioorthogonal conjugation. The DNA-nano-hydrogels revealed high specificity toward hybridization of complementary oligonucleotides, which allowed highly selective immobilization of DNA-labeled nonadherent Jurkat cells on the DNA-modified nanohydrogels with adjustable cell densities. The DNA-based cell-to-surface anchor could be specifically cleaved via the strand displacement mechanism using a nucleic acid competitor and resulting in the release of 75-95% of the anchored cells. The robustness of the surface immobilized nanohydrogels was demonstrated in a micro-patterning process. Employing digital projection photolithography on a positive-tone resist, the nanohydrogel networks could assemble in the shape defined microwells and retained the pattern fidelity as well as DNA-functionality after photoresist stripping, allowing spatially controlled DNA-assisted cell immobilization. The possibility of the micro-patterning as well as the dual properties, cell repelling if unmodified and cell attractive if specific cues were present, predestine the DNA-spider silk fibrillar networks for development of tunable biocompatible surfaces. The majority of materials used for cell patterning are based on the use of synthetic polymers specifically tailored to the selected patterning technique, especially when

immobilization of biologically active components is required.[56,57] As a result of this customization, these materials are chemically different from the bulk materials used in tissue engineering and implants in general,[58] making it difficult to directly link cell responses between microscopic and bulk platforms. In the case of the recombinant spider silk protein, the fibrous nature of bulk hydrogels,[59] reflecting the ECM matrix, has become the basis for biofabrication approaches in tissue engineering.[39,60,61] Here, we applied spider silk self-assembly using the fibrous, hydrogel-like morphology that persists on the surface[41,42] to expose specific biotargeting functions represented by DNA interactions as a model. Moreover, any insights gained on the microstructured platforms based on the presented nanohydrogels will facilitate and accelerate the transfer of knowledge toward bulk hydrogels suitable for 3D printing of scaffolds or coatings of implants. Further modifications of the proteinaceous platform, including fused enzymes,[35] factors, or peptide tags,[62] are likely possible to specify or modulate the chemical and biological responses of the fibrillar scaffold. The possibilities to micropattern as well as functionalize the protein-based nanohydrogel surfaces using the DNA-spider silk conjugates with aptameric functionality[63,64] would enable targeting of specific cell markers. Thus, further developments of spider silk nanohydrogels will enable their integration into platforms suitable for isolation of circulating cancer cells, single cell cloning in stem cell therapies, CRISPR-based genetic manipulations, or a production of protein therapeutics.

METHODS

If not stated otherwise, all chemicals were supplied by Merck KGaA (Germany) in analytical grade. Recombinant spider silk protein eADF4(C16) was prepared as published.65 Synthetic oligonucleotides were obtained from biomers.net (Germany). Ultrapure water in the experiments was obtained using a Millipore system (Merck KGaA).

Processing of Spider Silk Films. The recombinant spider silk protein eADF4(C16) was processed as described recently.42 The protein films in well-plates were drop-casted from a hexafluoroiso-propanol (HFIP) (abcr GmbH, Germany) solution at 1.6 mg/mL, and 100 μL/well were added into 96-well plates (F-Bottom, μClear, black, Cellstar, Greiner Bio-One International GmbH, Germany), resulting in 0.5 mg/cm^2 protein films.

For AFM imaging, Si-wafers were cleaned using the RCA procedure[41] and 100% O_2 plasma at 0.2 mbar for 1 min as well as silanized with (3-aminopropyl)triethoxysilane (APTES) vapors in a desiccator for 16 h. The APTES modified glass slides were annealed at 60 °C for 1 h. eADF4(C16) was dissolved in formic acid (10 mg/ mL), and 20 ^L of the protein solution was spin-coated (spin coater SCE-150, Schaefer Technologie GmbH, Germany) at 3 s acceleration and 4000 rpm for 30 s. To render the films in well-plates as well as on the Si-wafers water insoluble, samples were exposed to methanol vapors in a desiccator for 16 h.[66]

Self-Assembly of Nanohydrogels. Aqueous protein solutions were prepared upon a solubilization in 6 M GuaSCN and dialysis as described previously.[36] The protein solution was centrifuged at 55,000 rpm (centrifuge Optima MAX-XP, rotor TLA-55, Beckman Coulter Inc., USA) at 4 °C for 55 min. Using the eADF4(C16) films as a seeding surface, nanofibrillar networks were assembled on top using 2-10 μM unmodified, azido modified,[36] or DNA-conjugated eADF4(C16)[42] in 100 μM potassium phosphate, pH

8 in a humid chamber for 24 h and washed with 10 mM Tris/HCl, 100 μM NaCl, pH 8 before further modifications.

Azide-Alkyne Coupling. After the assembly of nanohydrogels from 10 μM N_3-eADF4(C16), commercially synthesized DBCO-DNAs (capture sequence (cap) ttttttattcctcgcctgtc and reporter sequence (rep) ttttttgacaggcgaggaat from ref 36 as well as mismatched sequences (**Figure S5**)) were incubated at different concentrations in 10 μM Tris/HCl, 100 mM NaCl, pH 8 at 37 °C using a humid chamber for different time periods, followed by washing three times with 10 μM Tris/HCl, 300 μM NaCl, pH 8. Functionalization of the nanohydrogels with the rep- or cap sequences was validated by the addition of 0.5 μM 5'-fluorescein labeled complementary DNA probes at 37 °C for 1 h followed by three washings with 10 μM Tris/ HCl, 300 μM NaCl, 5 mg/mL BSA, pH 8 and fluorescence scans in a plate reader (Mithras LB 940; Berthold Technologies GmbH, Germany). For further DNA-assisted cell immobilizations, coupling of DBCO-DNA in a concentration of 10 μM was performed with an incubation time of 72 h.

DNA-Labeling of Cells. 10^6 cells were washed, resuspended in PBS, and labeled by the addition of 0.520 μM DSL-rep (commercial 5'-distearoyl lipid modifier on rep sequence) or CHOP-rep (commercial 5'-cholesterol prolinol modifier on rep sequence) in a total volume of 50 μL. The cells were incubated with occasional gentle agitation for 5 min. The cells were washed three times with 1 mL of ice-cold PBS to remove the unbound DNA and stained in suspension using 0.3 μM calcein-AM, 0.3 μM DAPI and 0.5 μM TAMRA-cap before visualization in a fluorescence microscope (DMi8, Leica Microsystems GmbH, Germany). If not otherwise stated, 5 μM rep sequences were used for the cell membrane modifications and DNA-assisted immobilizations.

DNA-Assisted Immobilization of Cells. Rep-labeled cells were resuspended in RPMI-1640 medium, seeded at a density of 150,000 cells/cm^2 on the DNA-modified spider silk nanohydrogels, and incubated at 37 °C, 5% CO_2 in a humid atmosphere for at least 30 min. If not indicated otherwise, cells were simultaneously live-stained by the addition of 0.3 μM calcein-AM. Unbound cells were then removed by washing with PBS, and the remaining cells were visualized in medium using a fluorescence microscope (DMi8, Leica Microsystems GmbH, Germany). The cell densities in the fluorescence images were analyzed using a Fiji software (ImageJ, Open source). The image threshold of the FITC channel was adjusted to obtain as many separate cells as possible, and the average cell counts were obtained using a function "analyze particles" from three wells per experiment.

Cell Release. For microscopic analysis of the DNA strand displacement on cell surface, the DSL-rep modified cells were treated either with 5 μM 5'-TAMRA-cap oligonucleotide or with an equimolar mixture of TAMRA-cap and 5'-fluorescein labeled competitive sequence FAM-cap-comp sequence (ttattcctcgcctgt-caaaaaa) at 37 °C for 10 min. After washing with PBS, the cells were visualized using the fluorescence microscope.

To release the cells immobilized via cap/rep hybridization, 5 μM of FAM-cap-comp probe was added to the rep-cells on cap-nanohydrogels and incubated at 37 °C, 5% CO_2 for 30 min or longer time periods. Cells were washed subsequently with PBS and visualized in a medium using the fluorescence microscope.

Photolithographic Preparation of Microwells. Glass cover-slips (Ø 19 mm) were cleaned using acetone, isopropanol, and RCA procedure, before activation with 100% O_2-plasma (0.2 mbar for 1 min) and silanized using 0.1% (v/v) APTES in ethanol for 16 h.[67] The amino activated slides were prebaked at 120 °C for 10 min on a precision hot plate HP 60 (Torrey Pines Scientific, Inc., USA) to evaporate adsorbed H_2O. Thereafter the coverslips were placed onto a spin coater, and 55 μL of Ti-Prime (Microchemicals GmbH, Germany) was applied at 50 rps for 30 s with an acceleration time of 3 s. The coated plates were incubated 2 min at 120 °C on the hot plate and spin coated with 55 μL of the AZ 1512 HS positive photoresist (Microchemicals GmbH, Germany), resulting in a photoresist thickness of approximately 1 μm. After a postbake at 100 °C for 2 min, the coverslips were illuminated using a SmartPrint maskless lithography equipment based on a μLCD projection technology (Microlight3D, France) at 435 nm (10.2 mW-cm^{-2}) for 40 s. The microwells were developed in 1:4 (v/v) AZ 400 K developer (Microchemicals GmbH, Germany)/H2O solution using agitation for 30 s. To render the microstructures more resilient against longer incubations in aqueous media, hardening was conducted using exposure to a deep UV light (Benda NU-6 KL UV lamp) for 2.5 min following a hard bake at 130 °C for 5 min.

Nanohydrogel Assembly in Microwells. After the photolithography, the amino modified surface in the deprotected microwells was covalently modified in a solution of 2.5 μM eADF4(C16) and 2.5 mg/mL N-(3-dimethylaminopropyl)-N'-ethylcarbodiimid-hydro-chlorid (EDC) in 50 mM HEPES/Na, pH 7.1 for 16 h. Thereafter, the coverslips were washed with 50 mM HEPES pH 7.1 and incubated in a solution of 5 μM eADF4(C16) in 100 μM K-Pi, 50 mM HEPES pH 7.1 for 16 h. The coverslips were washed with 10 μM Tris/HCl, 100 mM NaCl, pH 8 and subsequently with Milli-Q H_2O.

Preparation of DNA-Nanohydrogel Patterned Surface. The assembled nanohydrogels were functionalized in the microwells with 5/-amino modified oligonucleotides (5 μM) and 5 mg/mL EDC in 50 mM HEPES pH 8 for 16 h. Thereafter, the substrates were washed with 10 μM Tris/HCl, 100 μM NaCl pH 7.5 and H2O. The photoresist was stripped off using a bright field lamp (Makita DEADML801) at the maximum intensity for 2 min followed by 10 min consecutive incubations in a solution of 1:4 (v/v) AZ 400 K developer/H_2O, 2:1 (v/v) acetone/ethyl acetate, acetone, and Milli-Q H_2O. The exposed amino groups were blocked with 5 μM NHS activated branched PEG[68] (methyl-$(PEG_{12})_3$-PEG_4-NHS ester, Thermo Fisher Scientific Inc., USA) in 50 μM HEPES pH 7.1 for 16 h, to gain antifouling properties of the photoresist free surface.

Cell Immobilization on the Nanohydrogel Pattern. The substrates with nanohydrogel pattern were sterilized in 70% ethanol for 10-20 min, washed 3X with PBS, and placed into a 12-well polystyrene cell culture plate (Nunc, ThermoSientific). 150,000 DSL-rep modified cells per cm^2 were seeded onto in the presence of 0.3 μM calcein-AM in RPMI-1640 medium at 37 °C, 5% CO_2 and a humid atmosphere for 1 h. Subsequently the supernatant was removed, and the coverslips were washed 3X with cold PBS. Medium was then applied in case of fluorescence microscopy imaging or 70% EtOH for a fixation in case of AFM scanning.

Statistical Analysis If not indicated otherwise, the experimental data were evaluated using the arithmetic mean and standard deviation of triplicates. Comparisons of multiple sample groups were statistically assessed using a one-way ANOVA test in the software Origin (OriginLab Corporation, USA). Data were considered as statistically significant if $p < 0.05$. Fluorescence intensities obtained in flow cytometry experiments, which histograms predominantly show an asymmetric non-normal distribution of the populations, were evaluated by the median, representing a more robust estimation to statistical outliers.[69]

REFERENCES

(1) Gomes, S.; Leonor, I. B.; Mano, J. F.; Reis, R. L.; Kaplan, D. L. Natural and Genetically Engineered Proteins for Tissue Engineering. Prog. Polym. Sci. **2012**, 37, 1 — 17.

(2) Okamoto, M.; John, B. Synthetic Biopolymer Nanocomposites for Tissue Engineering Scaffolds. Prog. Polym. Sci. **2013**, 38, 1487— 1503.

(3) Oliveira, M. B.; Mano, J. F. High-Throughput Screening for Integrative Biomaterials Design: Exploring Advances and New Trends. Trends Biotechnol. **2014**, 32, 627—636.

(4) Yliperttula, M.; Chung, B. G.; Navaladi, A.; Manbachi, A.; Urtti, A. High-Throughput Screening of Cell Responses to Biomaterials. Eur. J. Pharm. Sci. **2008**, 35, 151 — 160.

(5) Simon, C. G., Jr.; Lin-Gibson, S. Combinatorial and High-Throughput Screening of Biomaterials. Adv. Mater. **2011**, 23, 369— 387.

(6) Yang, L.; Pijuan-Galito, S.; Rho, H. S.; Vasilevich, A. S.; Eren, A. D.; Ge, L.; Habibovic, P.; Alexander, M. R.; de Boer, J.; Carlier, A.; van Rijn, P.; Zhou, Q. High-Throughput Methods in the Discovery and Study of Biomaterials and Materiobiology. Chem. Rev. **2021**, 121, 4561—4677.

(7) Tronser, T.; Popova, A. A.; Levkin, P. A. Miniaturized Platform for High-Throughput Screening of Stem Cells. Curr. Opin. Biotechnol. **2017**, 46, 141—149.

(8) Harkness, T.; McNulty, J. D.; Prestil, R.; Seymour, S. K.; Klann, T.; Murrell, M.; Ashton, R. S.; Saha, K. High-Content Imaging with Micropatterned Multiwell Plates Reveals Influence of Cell Geometry and Cytoskeleton on Chromatin Dynamics. Biotechnol. J. **2015**, 10, 1555—1567.

(9) Yoshii, Y.; Furukawa, T.; Waki, A.; Okuyama, H.; Inoue, M.; Itoh, M.; Zhang, M.-R.; Wakizaka, H.; Sogawa, C.; Kiyono, Y.; Yoshii, H.; Fujibayashi, Y.; Saga, T. High-Throughput Screening with Nanoimprinting 3d Culture for Efficient Drug Development by Mimicking the Tumor Environment. Biomaterials **2015**, 51, 278—289.

(10) Anderson, D. G.; Levenberg, S.; Langer, R. Nanoliter-Scale Synthesis of Arrayed Biomaterials and Application to Human Embryonic Stem Cells. Nat. Biotechnol **2004**, 22, 863-866.

(11) Flaim, C. J.; Chien, S.; Bhatia, S. N. An Extracellular Matrix Microarray for Probing Cellular Differentiation. Nat. Meth. , 2, 119-125.

(12) Gobaa, S.; Hoehnel, S.; Roccio, M.; Negro, A.; Kobel, S.; Lutolf, M. P. Artificial Niche Microarrays for Probing Single Stem Cell Fate in High Throughput. Nat. Meth. **2011**, 8, 949-955.

(13) Beachley, V. Z.; Wolf, M. T.; Sadtler, K.; Manda, S. S.; Jacobs, H.; Blatchley, M. R.; Bader, J. S.; Pandey, A.; Pardoll, D.; Elisseeff, J. H. Tissue Matrix Arrays for High-Throughput Screening and Systems Analysis of Cell Function. Nat. Meth. **2015**, 12, 1197-1204.

(14) Dirscherl, C.; Springer, S. Protein Micropatterns Printed on Glass: Novel Tools for Protein-Ligand Binding Assays in Live Cells. Eng. Life Sci **2018**, 18, 124-131.

(15) Chen, L.; Yan, C.; Zheng, Z. Functional Polymer Surfaces for Controlling Cell Behaviors. Mater. Today **2018**, 21, 38-59.

(16) Chiang, E. N.; Dong, R.; Ober, C. K.; Baird, B. A. Cellular Responses to Patterned Poly(Acrylic Acid) Brushes. Langmuir **2011**, 27, 7016-7023.

(17) Sevcsik, E.; Brameshuber, M.; Folser, M.; Weghuber, J.; Honigmann, A.; Schutz, G. J. Gpi-Anchored Proteins Do Not Reside in Ordered Domains in the Live Cell Plasma Membrane. Nat. Commun. **2015**, 6, 6969.

(18) Barata, D.; van Blitterswijk, C.; Habibovic, P. High-Throughput Screening Approaches and Combinatorial Development of Biomaterials Using Microfluidics. Acta Biomater. **2016**, 34, 120.

(19) Suri, S.; Singh, A.; Nguyen, A. H.; Bratt-Leal, A. M.; McDevitt, T. C.; Lu, H. Microfluidic-Based Patterning of Embryonic Stem Cells for in Vitro Development Studies. Lab Chip **2013**, 13, 46174624.

(20) Yarmush, M. L.; King, K. R. Living-Cell Microarrays. Annu. Rev. Biomed. Eng. **2009**, 11, 235-257.

(21) Tourniaire, G.; Collins, J.; Campbell, S.; Mizomoto, H.; Ogawa, S.; Thaburet, J.-F.; Bradley, M. Polymer Microarrays for Cellular Adhesion. Chem. Commun. (Camb.) **2006**, 2118-2120.

(22) Date, A.; Pasini, P.; Daunert, S. Fluorescent and Bioluminescent Cell-Based Sensors: Strategies for Their Preservation. In Whole Cell Sensing Systems I: Reporter Cells and Devices; Belkin, S., Gu, M. B., Eds.; Springer: Berlin, Heidelberg, **2010**; pp 57-75.

(23) Vermesh, U.; Vermesh, O.; Wang, J.; Kwong, G. A.; Ma, C.; Hwang, K.; Heath, J. R. High-Density, Multiplexed Patterning of Cells at Single-Cell Resolution for Tissue Engineering and Other Applications. Angew. Chem., Int. Ed. **2011**, 50, 7378-7380.

(24) Meyer, R.; Giselbrecht, S.; Rapp, B. E.; Hirtz, M.; Niemeyer, C. M. Advances in DNA-Directed Immobilization. Curr. Opin. Chem. Biol. **2014**, 18, 8-15.

(25) Schneider, A.-K.; Niemeyer, C. M. DNA Surface Technology -from Gene Sensors to Integrated Systems for Life Science and Materials Research. Angew. Chem., Int. Ed. **2018**, 57, 1695916967.

(26) Scheideler, O. J.; Yang, C.; Kozminsky, M.; Mosher, K. I.; Falcón-Banchs, R.; Ciminelli, E. C.; Bremer, A. W.; Chern, S. A.; Schaffer, D. V.; Sohn, L. L. Recapitulating Complex Biological Signaling Environments Using a Multiplexed, DNA-Patterning Approach. Science Advances **2020**, 6, No. eaay5696.

(27) Chen, S.; Bremer, A. W.; Scheideler, O. J.; Na, Y. S.; Todhunter, M. E.; Hsiao, S.; Bomdica, P. R.; Maharbiz, M. M.; Gartner, Z. J.; Schaffer, D. V. Interrogating Cellular Fate Decisions with High-Throughput Arrays of Multiplexed Cellular Communities. Nat. Commun. **2016**, 7, 10309.

(28) Hsiao, S. C.; Shum, B. J.; Onoe, H.; Douglas, E. S.; Gartner, Z. J.; Mathies, R. A.; Bertozzi, C. R.; Francis, M. B. Direct Cell Surface Modification with DNA for the Capture of Primary Cells and the Investigation of Myotube Formation on Defined Patterns. Langmuir **2009**, 25, 6985-6991.

(29) Todhunter, M. E.; Jee, N. Y.; Hughes, A. J.; Coyle, M. C.; Cerchiari, A.; Farlow, J.; Garbe, J. C.; LaBarge, M. A.; Desai, T. A.; Gartner, Z. J. Programmed Synthesis of Three-Dimensional Tissues. Nat. Meth. **2015**, 12, 975-981.

(30) Ling, S.; Chen, W.; Fan, Y.; Zheng, K.; Jin, K.; Yu, H.; Buehler, M. J.; Kaplan, D. L. Biopolymer Nanofibrils: Structure, Modeling, Preparation, and Applications. Prog. Polym. Sci. **2018**, 85, 156.

(31) Ling, S.; Kaplan, D. L.; Buehler, M. J. Nanofibrils in Nature and Materials Engineering. Nat. Rev. Mater. **2018**, 3, 18016.

(32) Zhang, Y. S.; Khademhosseini, A. Advances in Engineering Hydrogels. Science **2017**, 356, No. eaaf3627.

(33) Humenik, M.; Magdeburg, M.; Scheibel, T. Influence of Repeat Numbers on Self-Assembly Rates of Repetitive Recombinant Spider Silk Proteins. J. Struct. Biol. **2014**, 186, 431-437.

(34) Humenik, M.; Smith, A. M.; Arndt, S.; Scheibel, T. Ion and Seed Dependent Fibril Assembly of a Spidroin Core Domain. J. Struct. Biol. **2015**, 191, 130-138.

(35) Humenik, M.; Mohrand, M.; Scheibel, T. Self-Assembly of Spider Silk-Fusion Proteins Comprising Enzymatic and Fluorescence Activity. Bioconjugate Chem. **2018**, 29, 898-904.

(36) Humenik, M.; Scheibel, T. Nanomaterial Building Blocks Based on Spider Silk-Oligonucleotide Conjugates. ACS Nano **2014**, 8, 1342-1349.

(37) Humenik, M.; Drechsler, M.; Scheibel, T. Controlled Hierarchical Assembly of Spider Silk-DNA Chimeras into Ribbons and Raft-Like Morphologies. Nano Lett. **2014**, 14, 3999-4004.

(38) Zeplin, P. H.; Maksimovikj, N. C.; Jordan, M. C.; Nickel, J.; Lang, G.; Leimer, A. H.; Romer, L.; Scheibel, T. Spider Silk Coatings as a Bioshield to Reduce Periprosthetic Fibrous Capsule Formation. Adv. Funct. Mater. **2014**, 24, 2658-2666.

(39) Steiner, D.; Winkler, S.; Heltmann-Meyer, S.; Trossmann, V. T.; Fey, T.; Scheibel, T.; Horch, R. E.; Arkudas, A. Enhanced Vascularization and De Novo Tissue Formation in Hydrogels Made of Engineered Rgd-Tagged Spider Silk Proteins in the Arteriovenous Loop Model. Biofabrication **2021**, 13, No. 045003.

(40) Aigner, T. B.; DeSimone, E.; Scheibel, T. Biomedical Applications of Recombinant Silk-Based Materials. Adv. Mater. **2018**, 30, 1704636.

(41) Molina, A.; Scheibel, T.; Humenik, M. Nanoscale Patterning of Surfaces Via DNA Directed Spider Silk Assembly. Biomacromolecules **2019**, 20, 347-352.

(42) Humenik, M.; Preifí, T.; Godrich, S.; Papastavrou, G.; Scheibel, T. Functionalized DNA-Spider Silk Nanohydrogels for Controlled Protein Binding and Release. Mater. Today Bio **2020**, 6, 100045.

(43) Agard, N. J.; Prescher, J. A.; Bertozzi, C. R. A Strain-Promoted 3 + 2 Azide-Alkyne Cycloaddition for Covalent Modification of Biomolecules in Living Systems. J. Am. Chem. Soc. **2004**, 126, 1504615047.

(44) Liu, H.; Kwong, B.; Irvine, D. J. Membrane Anchored Immunostimulatory Oligonucleotides for in Vivo Cell Modification and Localized Immunotherapy. Angewandte Chemie (International ed. in English) **2011**, 50, 7052-7055.

(45) Weber, R. J.; Liang, S. I.; Selden, N. S.; Desai, T. A.; Gartner, Z. J. Efficient Targeting of Fatty-Acid Modified Oligonucleotides to Live Cell Membranes through Stepwise Assembly. Biomacromolecules **2014**, 15, 4621-4626.

(46) Bagheri, Y.; Chedid, S.; Shafiei, F.; Zhao, B.; You, M. A Quantitative Assessment of the Dynamic Modification of Lipid-DNA Probes on Live Cell Membranes. Chemical science **2019**, 10, 1103011040.

(47) Zhao, B.; Tian, Q.; Bagheri, Y.; You, M. Lipid-Oligonucleotide Conjugates for Simple and Efficient Cell Membrane Engineering and Bioanalysis. Current opinion in biomedical engineering **2020**, 13, 76.

(48) McGinnis, C. S.; Patterson, D. M.; Winkler, J.; Conrad, D. N.; Hein, M. Y.; Srivastava, V.; Hu, J. L.; Murrow, L. M.; Weissman, J. S.; Werb, Z.; Chow, E. D.; Gartner, Z. J. Multi-Seq: Sample Multiplexing for Single-Cell Rna Sequencing Using Lipid-Tagged Indices. Nat. Methods **2019**, 16, 619-626.

(49) Audiffred, J. F.; De Leo, S. E.; Brown, P. K.; Hale-Donze, H.; Monroe, W. T. Characterization and Applications of Serum-Free Induced Adhesion in Jurkat Suspension Cells. Biotechnol. Bioeng. **2010**, 106, 784-793.

(50) Platnich, C. M.; Hariri, A. A.; Rahbani, J. F.; Gordon, J. B.; Sleiman, H. F.; Cosa, G. Kinetics of Strand Displacement and Hybridization on Wireframe DNA Nanostructures: Dissecting the Roles of Size, Morphology, and Rigidity. ACS Nano **2018**, 12, 1283612846.

(51) Tidd, D. M.; Warenius, H. M. Partial Protection of Oncogene, Anti-Sense Oligodeoxynucleotides against Serum Nuclease Degradation Using Terminal Methylphosphonate Groups. Br. J. Cancer **1989**, 60, 343-350.

(52) von Kockritz-Blickwede, M.; Chow, O. A.; Nizet, V. Fetal Calf Serum Contains Heat-Stable Nucleases That Degrade Neutrophil Extracellular Traps. Blood **2009**, 114, 5245-5246.

(53) Mohrle, B. P.; Kohler, K.; Jaehrling, J.; Brock, R.; Gauglitz, G. Label-Free Characterization of Cell Adhesion Using Reflectometric Interference Spectroscopy (Rifs). Anal. Bioanal. Chem. **2005**, 384, 407-413.

(54) Salazar-Fontana, L. I.; Barr, V.; Samelson, L. E.; Bierer, B. E. Cd28 Engagement Promotes Actin Polymerization through the Activation of the Small Rho Gtpase Cdc42 in Human T Cells. Journal of immunology **2003**, 171, 2225-2232.

(55) Lamerton, R. E.; Lightfoot, A.; Nieves, D. J.; Owen, D. M. The Role of Protein and Lipid Clustering in Lymphocyte Activation. Frontiers in Immunology 2021, 12, 600961 DOI: **10.3389/ fimmu.2021.600961**.

(56) Humenik, M.; Winkler, A.; Scheibel, T. Patterning of Protein-Based Materials. Biopolymers **2021**, 112, No. e23412.

(57) Mertgen, A.-S.; Trossmann, V. T.; Guex, A. G.; Maniura-Weber, K.; Scheibel, T.; Rottmar, M. Multifunctional Biomaterials: Combining Material Modification Strategies for Engineering of CellContacting Surfaces. ACS Appl Mater. Interfaces **2020**, 12, 2134221367.

(58) Park, S.-B.; Lih, E.; Park, K.-S.; Joung, Y. K.; Han, D. K. Biopolymer-Based Functional Composites for Medical Applications. Prog. Polym. Sci **2017**, 68, 77-105.

(59) Schacht, K.; Scheibel, T. Controlled Hydrogel Formation of a Recombinant Spider Silk Protein. Biomacromolecules **2011**, 12, 24882495.

(60) Kumari, S.; Lang, G.; DeSimone, E.; Spengler, C.; Trossmann, V. T.; Lucker, S.; Hudel, M.; Jacobs, K.; Kramer, N.; Scheibel, T. Engineered Spider Silk-Based 2d and 3d Materials Prevent Microbial Infestation. Mater. Today **2020**, 41, 21-33.

(61) Lechner, A.; Trossmann, V. T.; Scheibel, T. Impact of Cell Loading of Recombinant Spider Silk Based Bioinks on Gelation and Printability. Macromol. Biosci. **2022**, 22, 2100390.

(62) Wohlrab, S.; Muller, S.; Schmidt, A.; Neubauer, S.; Kessler, H.; Leal-Egana, A.; Scheibel, T. Cell Adhesion and Proliferation on Rgd-Modified Recombinant Spider Silk Proteins. Biomaterials **2012**, 33, 6650-6659.

(63) Soldevilla, M. M.; Villanueva, H.; Pastor, F. Aptamers as a Promising Therapeutic Tool for Cancer Immunotherapy. In Immunotherapy - Myths, Reality, Ideas, Future; Metodiev, K., Ed.; IntechOpen: London, **2017**; pp 129-150.

(64) Mercier, M.-C.; Dontenwill, M.; Choulier, L. Selection of Nucleic Acid Aptamers Targeting Tumor Cell-Surface Protein Biomarkers. Cancers **2017**, 9, 69.

(65) Huemmerich, D.; Helsen, C. W.; Quedzuweit, S.; Oschmann, J.; Rudolph, R.; Scheibel, T. Primary Structure Elements of Spider Dragline Silks and Their Contribution to Protein Solubility. Biochemistry **2004**, 43, 13604-13612.

(66) Borkner, C. B.; Lentz, S.; Muller, M.; Fery, A.; Scheibel, T. Ultra-Thin Spider Silk Films: Insights into Spider Silk Assembly on Surfaces. ACS Applied Polymer Materials **2019**, 1, 3366-3374.

(67) Miranda, A.; Martinez, L.; De Beule, P. A. A. Facile Synthesis of an Aminopropylsilane Layer on Si/Sio2 Substrates Using Ethanol as Aptes Solvent. MethodsX **2020**, 7, 100931.

(68) Chen, Q.; Yu, S.; Zhang, D.; Zhang, W.; Zhang, H.; Zou, J.; Mao, Z.; Yuan, Y.; Gao, C.; Liu, R. Impact of Antifouling Peg Layer on the Performance of Functional Peptides in Regulating Cell Behaviors. J. Am. Chem. Soc. **2019**, 141, 16772-16780.

(69) Cossarizza, A.; Chang, H.-D.; Radbruch, A.; Akdis, M.; Andra, I.; Annunziato, F.; Bacher, P.; Barnaba, V.; Battistini, L.; Bauer, W. M.; Baumgart, S.; Becher, B.; Beisker, W.; Berek, C.; Blanco, A.; Borsellino, G.; Boulais, P. E.; Brinkman, R. R.; Buscher, M.; Busch, D. H.; et al. Guidelines for the Use of Flow Cytometry and Cell Sorting in Immunological Studies*. Eur. J. Immunol. **2017**, 47, 1584-1797.